ACS Combinatorial Science

Research Article

pubs.acs.org/acscombsci

Optimization of the Single-Phased White Phosphor of Li_2SrSiO_4: Eu^{2+}, Ce^{3+} for Light-Emitting Diodes by Using the Combinatorial Approach Assisted with the Taguchi Method

Lei Chen,*[,†,∥] Anqi Luo,[†] Yao Zhang,[†] Fayong Liu,[†] Yang Jiang,[†] Qingsheng Xu,[†] Xinhui Chen,[†] Qingzhuo Hu,[†] Shi-Fu Chen,*[,‡] Kuo-Ju Chen,[§] and Hao-Chung Kuo[§]

[†]School of Materials Science and Engineering, Hefei University of Technology, Hefei 230009, China

[‡]Department of Chemistry, Huaibei Normal University, Huaibei 235000, China

[§]Department of Photonic & Institute of Electro-Optical Engineering, National Chiao Tung University, Hsinchu 30010, Taiwan

[∥]Semiconductor and Optoelectronic Technology Engineering Research Center of Anhui Province, Wuhu 241000, China

Supporting Information

ABSTRACT: The best performance of the phosphor Li_2SrSiO_4: Eu^{2+}, Ce^{3+} in terms of luminescence efficiency (LE), color rendering index (CRI) and color temperature (Tc) for light-emitting diode application was optimized with combinatorial approach. The combinatorial libraries were synthesized with solution-based method and the scale-up samples were synthesized with conventional solid-reaction method. Crystal structure was investigated by using the X-ray diffraction spectrometer. The emission spectra of each sample in combinatorial libraries were measured in situ by using a fiber optic spectrometer. Fluorescence spectrometers were used to record excitation and emission spectra of bulk samples. White light generation was tuned up by tailoring Eu^{2+} and Ce^{3+} concentrations in the single-phased host of Li_2SrSiO_4 under near-ultraviolet excitation, but it exhibited low efficiency of luminescence and poor color rendering index. The effects of each level of the Eu^{2+} and Ce^{3+} concentrations on LE, CRI, and Tc were evaluated with the Taguchi method. The optimum levels of the interaction pairs between Eu^{2+} and Ce^{3+} concentration on LE, CRI, and Tc were [2, 1] (0.006 M, 0.003 M), [1, 2] (0.003 M, 0.006 M), and [3, 1] (0.009 M, 0.00 3M), respectively. The thermal stability of luminescence, the external quantum efficiency (QE), luminance, chromaticity coordinates, correlated color temperature, color purity including the composition ratio of RGB in white light, and color rendering index of the white light emission of phosphor were evaluated comprehensively from a bulk sample.

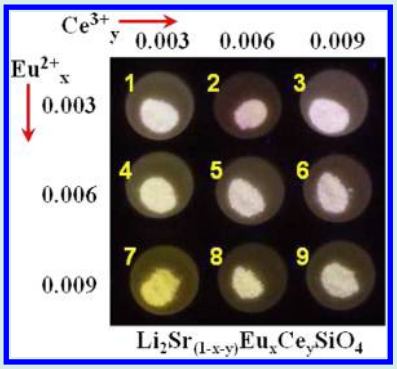

KEYWORDS: *white light-emitting diodes, luminescence, phosphor, Li_2SrSiO_4: Eu^{2+}, Ce^{3+}, combinatorial approach, the Taguchi method*

1. INTRODUCTION

White light-emitting-diodes (WLEDs) were considered as a new generation of green and energy-saving light source, owning small solid volume and strong ability to endure serious shock with high reliability.[1−4] For this reason, many efforts have been paid to replace the conventional compact fluorescent lamps with WLEDs.[5−8] Nevertheless, the white light was mainly produced by a combination of blue light from an InGaN LED chip and excited emission from the yellow phosphor of $Y_3Al_5O_{12}$:Ce^{3+} (YAG) or by exciting three-primary phosphors with near-ultraviolet (NUV) emission of LEDs at present.[9,10] As for the YAG-based WLEDs, the blue emission of LED chips depends strongly on current strength, which will result in the luminescence color of WLEDs shift with current fluctuations, occasionally yellowish or partially bluish. As for the tricolor-phosphor-type WLEDs, the deposition, segregation, and inhomogeneous distribution of various phosphors because of their different particle sizes and densities will affect the luminescence color and efficiency of WLEDs.[11] In view of these aspects, a single host activated with multiactivators which can emit white light was desired for WLEDs, especially those containing red composition with high CRI.[12,13]

The orange-yellow emission of Li_2SrSiO_4:Eu^{2+} was first reported by Varadaraju,[14] and the improvement of red emission compared to the commercial YAG:Ce phosphor was obtained by coating the phosphor of Li_2SrSiO_4:Eu^{2+} on an InGaN LED chip (max = 420 nm).[14] The yellow, yellow green, pure green and bluish green luminescence were observed in the ternary composition library of Li_2SrSiO_4:Eu^{2+}−Li_2BaSiO_4:Eu^{2+}−Li_2CaSiO_4:Eu^{2+}, including those unitary, binary, and mixtures, but in terms of both emission intensity and color chromaticity for WLEDs, the binary green phosphors with specific composition of $Li_2(Ba_{1-x}Sr_x)SiO_4$:Eu^{2+} ($0.28 < x < 0.56$) showed the best performance.[15] Moreover, the phosphor of

Received: June 4, 2012
Revised: September 23, 2012
Published: October 25, 2012

   dx.doi.org/10.1021/co300058x | *ACS Comb. Sci.* 2012, 14, 636−644

$Li_2SrSiO_4:Ce^{3+}$ displays blue emission.[16] Therefore, it is promising to produce white light by mixing the blue luminescence of Ce^{3+} with the orange emission of Eu^{2+}.[14−17] Zou's[17] research work has suggested that $Li_2SrSiO_4:Eu^{2+}$, Ce^{3+} could be a potential phosphor for WLED under NUV excitation and the intensity of luminescence maximized at x = 0.075 for $Li_2SrSiO_4:0.01Eu^{2+}\cdot xCe^{3+}$. However, more details about the feasibility of the phosphor for LEDs application, such as, the relation about LE, CRI, Tc, chromaticity coordinates CIE(x, y), and the concentrations of Eu^{2+} and Ce^{3+} with precise control levels, were not evaluated.

Combinatorial chemistry approach, which was initially developed to accelerate drug discovery, emerged as a technique for rapid synthesis and high-throughput screening of huge numbers of diverse compounds to search for new materials.[18−24] Nevertheless, even the largest combinatorial libraries that could be synthesized and screened only cover a small space of the well-known or unknown compounds.[25−30] To reduce the cost and time expended in the synthesis and characterization of innumerous compounds, some algorithms, including genetic, Monte Carlo techniques, simulated annealing guided evaluation, and artificial neural networks algorithms, have been adopted to compensate for the weakness of the combinatorial approach.[25−30] Undeniably, the application of algorithms in combinatorial approach has accelerated the discovery of new compounds, including biological targets, proteins, and nucleic acids.[25−30] As for inorganic phosphors, Sohn et al. employed the genetic algorithms, based on a global optimization strategy in which the evolutionary process is imitated with elitism, selection, crossover and random mutation operations, in the combinatorial approach to search for new luminescent materials for light-emitting diodes and plasma display panels.[31−33] The authors' previous research demonstrated that the performance of the combinatorial approach in evaluating the effects of components on an objective property, identifying the factors which one has the strongest effect and which one has minor effect, reducing the experimental dimensions of multifactors and estimating the expected performance under the optimal conditions, could be improved by combining with the Taguchi method.[34] Here, the method was further applied to optimize the white emission of $Li_2SrSiO_4:Eu^{2+}$, Ce^{3+} phosphor for WLEDs.

2. EXPERIMENTAL PROCEDURES

The experimental design and data analysis carried out with the Taguchi method were proceeded automatically with the aid of a computer by using the software of Qualitek-4.[38] The combinatorial libraries were synthesized by inkjetting precursor solutions into array wells on an Al_2O_3 substrate in the sequence of Sr → Si → Li → Ce → Eu for no less than three times, in a manner similar to that in refs 12 and 35. In our previous researchs, a reactor array containing about 11 × 11 wells with a diameter of 4 mm were used, but the experimental errors and consistency were hard to control for trace amounts of samples synthesized.[36,37] Here, the reactor array about 6 × 6 wells with a diameter of 8 mm was adopted. Sr^{2+}, Ce^{3+}, and Eu^{3+} solutions were prepared by dissolving due amount of $LiNO_3$, $Sr(NO_3)_2$, $Ce(NO_3)_3$, and $Eu(NO_3)_3$ into deionized water, respectively; the silicon sol was prepared by hydrolyzing ethyl silicate tetraethyl orthosilicate (TEOS) in deionized water. 5% excess Li^+ was added to compensate its evaporation during high temperature sintering. After it was dried at 100−120 °C, the microreactors that contained the precursors were first presintered at 600 °C for 2 h in the air, and then cooled down to room temperature with the furnace. Next, the prefired samples were pulverized with a quartz pestle. Finally, the combinatorial libraries were sintered at 850 °C for 4 h in the reducing atmosphere of 10% H_2 + 90% N_2 to yield the desired samples. The pictures of the overall luminescence of samples in combinatorial libraries were taken by using a digital camera excited with a potable Hg lamp. The emission spectra of each sample in reactor array were collected in situ with a fiber optic spectrometer (Ocean Optics, Inc., USB4000-UV−vis-ES). By taking samples out from reactors, the excitation and emission spectra were measured with Hitachi F4500 spectrometer. Meanwhile, crystal structure was investigated by using X-ray diffraction (XRD) spectrometer (Rigaku, D/Max-rB) with Cu Ka radiation (λ = 1.5418 Å). Some scale-up samples were synthesized with the conventional solid state reaction method. The thermal stability of luminescence, relative luminance, the external quantum efficiency (QE), color chromaticity, Tc, CRI, color purity, and the ratio of RBG in white light of luminescence of bulk samples were characterized by using the EVERFINE EX-1000 spectrometer.

3. RESULT AND DISCUSSION

In case of not knowing about the ideal concentrations of Eu^{2+} and Ce^{3+} for producing white light, a combinatorial library with a larger concentration range of activators was synthesized first. Figure 1 presents composition maps and luminescence

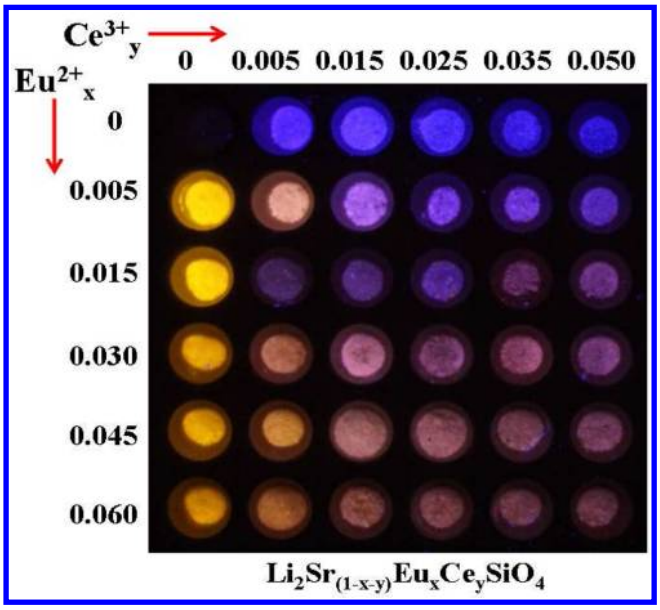

Figure 1. Composition map and luminescence photograph of the $Li_2(Sr_{1-x-y}Eu_xCe_y)SiO_4$ combinatorial library.

photograph of the $Li_2(Sr_{1-x-y}Eu_xCe_y)SiO_4$ combinatorial library under 365 nm excitation. As for the first sample in the top-left corner of the combinatorial library, no luminescence were observed from the host of Li_2SrSiO_4 for no Eu^{2+} and Ce^{3+} doping (x = 0 and y = 0). However, bright yellow luminescence is observed in the first longitudinal column with x = 0.005−0.060 and y = 0, and the luminance decreases with Eu^{2+} increasing from x = 0.005 to x = 0.060 step by step. When the concentration of Eu^{2+} is higher than 0.015 M, the luminescence decreases severely with its content increase. Similarly, bright blue emission was observed in the first

dx.doi.org/10.1021/co300058x | ACS Comb. Sci. 2012, 14, 636−644

transverse column with $x = 0$ and $y = 0.005-0.050$. From the picture, it is difficult to discriminate the difference of luminance within the concentration range of $y = 0.005$, 0.015, and 0.025 M for Ce^{3+}, but the luminescence intensity decreases significantly when Ce^{3+} concentration is higher than 0.025 M. The emission spectra of each sample in the first longitudinal column and those in the first transverse column of combinatorial library were provided in Supporting Information Figures 1 and 2, respectively. A broad emission band with peaks at about 418 and 570 nm were observed, which were attributed to the $4f^05d^1 \rightarrow 4f^1$ transition of Ce^{3+} and the $4f^65d^1 \rightarrow 4f^7$ transition of Eu^{2+}, respectively. Figure 2 presents the emission spectra of samples

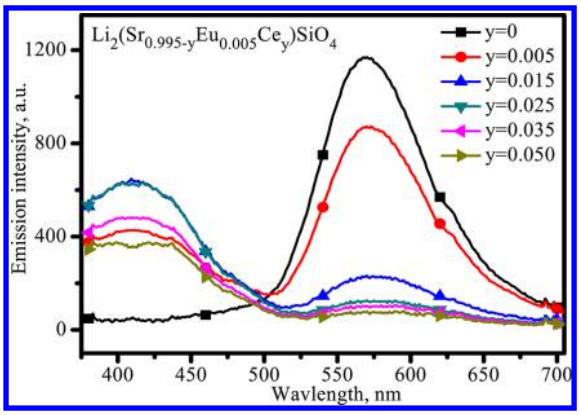

Figure 2. Emission spectra of $Li_2(Sr_{1-x-y}Eu_xCe_y)SiO_4$ ($x = 0.005$ and $y = 0$, 0.005, 0.015, 0.025, 0.035, and 0.050), corresponding to the second transverse column samples in Figure 1.

in the second transverse column of the combinatorial library. The spectra consist of both Eu^{2+} and Ce^{3+} emissions. The luminescence intensity of Ce^{3+} increases with its concentration initially from $y = 0$, maximizes at about $y = 0.005-0.015$ M, then decreases with Ce^{3+} content increasing further, but the luminescence intensity of Eu^{2+} decreases continuously with Ce^{3+} concentration increasing from 0 to 0.050 M. As revealed by the Supporting Information Figure 3, the overall luminescence intensity including both Eu^{2+} and Ce^{3+} emission achieved by integrating from 380 to 700 nm in Figure 2, increases as Ce^{3+} concentration increases from $y = 0$, maximizes at $y = 0.005$, and then decreases seriously with the increase of Ce^{3+} concentration,.

Figure 3 presents the XRD patterns of four samples of $Li_2(Sr_{1-x-y}Eu_xCe_y)SiO_4$ ($x = 0$, $y = 0$; $x = 0.06$, $y = 0$; $x = 0$, $y = 0.05$; and $x = 0.06$, $y = 0.05$) in the corner of combinatorial library in Figure 1. The four samples exhibit the same diffraction peaks, which can be indexed to the phase of Li_2SrSiO_4 (ICSD 16-7334), and no other phases including Eu, Ce, or other species were detected. Therefore, samples were well synthesized in this work and the activators of Eu^{2+} and Ce^{3+} ions have entered into the crystal lattice of Li_2SrSiO_4. Li_2SrSiO_4 crystallizes as a hexagonal structure with a space group of $P3_121$ and lattice constants of $a = 5.0228$ (0) Å, $c = 12.4552$ (1) Å, $c/a = 2.4797$, V (cell volume) = 272.13 (0) Å^3, and $z = 3$. Since the ionic radius of Eu^{2+} (1.09) and Ce^{3+} (1.03) are approximate to Sr^{2+} (1.12) but much larger than those of Li^+ (0.68) and Si^{4+} (0.42), Eu^{2+}, and Ce^{3+} should preferably occupy the site of Sr^{2+} in the crystal lattice of Li_2SrSiO_4. The framework of Li_2SrSiO_4 crystal structure is formed by connecting SiO_4 and LiO_4 tetrahedron with Sr^{2+} ions, where two SiO_4 and LiO_4 tetrahedrons share a common oxygen atom.

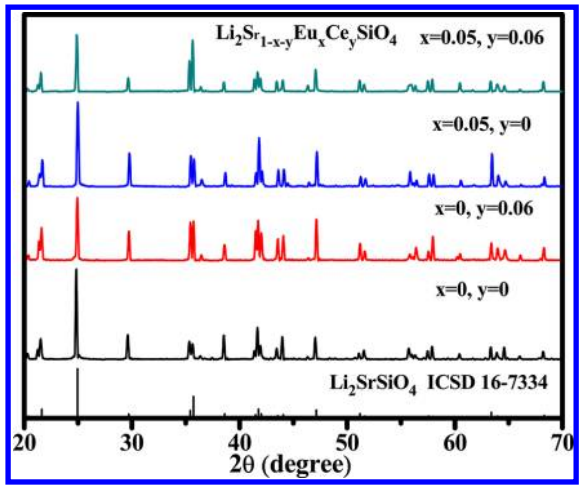

Figure 3. XRD patterns of $Li_2(Sr_{1-x-y}Eu_xCe_y)SiO_4$ ($x = 0$, $y = 0$; $x = 0.06$, $y = 0$; $x = 0$, $y = 0.05$; and $x = 0.06$, $y = 0.05$) compared with the standard ICSD 16-7334.

There is only one kind of site for Sr^{2+} ions surrounded by 8 oxygen atoms. The three-dimensional crystal structure of Li_2SrSiO_4 which is drawn according to ICSD 16-7334 is displayed in Supporting Information Figure 4.

Figure 1 demonstrates that different emission color could be tuned up by changing Eu^{2+} and Ce^{3+} alternatively in Li_2SrSiO_4. However, the luminance seemingly decreases seriously with the increase of Eu^{2+} and Ce^{3+} contents, especially when the concentrations of Eu^{2+} and Ce^{3+} are higher than 0.015 M. Thereby, it can be concluded that the reasonable concentration for both Eu^{2+} and Ce^{3+} to achieve efficient emission should not exceed 0.015 M. To obtain highly efficient white light generation, thus, a second combinatorial library was synthesized.

The experimental design and analysis were dealt with the Taguchi method.[34] In this study, two factors each with three levels of concentration, which are 1 (0.003 M), 2 (0.006 M), and 3 (0.009 M) for both Eu^{2+} and Ce^{3+}, were to be optimized. Therefore, the L-9 ($_3^4$) orthogonal array, which can accommodate four factors each with three levels, was selected to perform this experiment. The first and the second columns in the L-9 orthogonal array were set for the factors of Eu^{2+} and Ce^{3+}, respectively, and the third and the fourth columns were used to accommodate the interaction between the first and the second columns. Table 1 gives the experimental design, in which the 9 trial conditions represent the composition of the 9 samples to be optimized. The 9 samples were collected in a combinatorial library, synthesized with the same method as above.

Figure 4a displays the composition map and luminescence picture of the combinatorial library. Intuitively, white luminescence was tuned up within the concentration range of 0.003–0.009 M. Settled the concentration of Ce^{3+} at 0.003 M, the luminescence color of phosphors become yellowish as Eu^{2+} concentration increases from 0.003 through 0.006 to 0.009 M, seen from the first longitudinal column. Likewise, the emission color becomes bluish as Ce^{3+} concentration increases from 0.003 through 0.006 to 0.009 M when the concentration of Eu^{2+} is fixed to 0.003 M, displayed in the first traverse in Figure 4a. Figure 4b, c, and d presents the emission spectra of the 9 samples in the order of Eu^{2+} concentration increase and fixed the concentration of Ce^{3+} at $y = 0.003$, 0.006, and 0.009 for

dx.doi.org/10.1021/co300058x | ACS Comb. Sci. 2012, 14, 636–644

Table 1. Experimental Design and Results

experimental design					experimental results				
orthogonal array type L9(3^4)									
columns	1	2	3	4	CIE				
factors	Eu^{2+}	Ce^{3+}	inter cols 2 × 1	inter cols 2 × 1	*x*	*y*	Tc (K)	CRI (Ra)	external QE (%)
experiment 1	0.003	0.003	Lev-1	Lev-1	0.3924	0.3723	3648	62.7	24.459
experiment 2	0.003	0.006	Lev-2	Lev-2	0.3459	0.2904	4613	69.4	24.187
experiment 3	0.003	0.009	Lev-3	Lev-3	0.3578	0.3143	4243	67.1	27.539
experiment 4	0.006	0.003	Lev-2	Lev-3	0.3716	0.3508	4058	64.9	31.46
experiment 5	0.006	0.006	Lev-3	Lev-1	0.3738	0.351	3988	64.8	19.32
experiment 6	0.006	0.009	Lev-1	Lev-2	0.3714	0.331	3881	64.5	20.5
experiment 7	0.009	0.003	Lev-3	Lev-2	0.4377	0.4417	3272	57.9	17.441
experiment 8	0.009	0.006	Lev-1	Lev-3	0.4013	0.3839	3533	60.4	18.889
experiment 9	0.009	0.009	Lev-2	Lev-1	0.3845	0.363	3776	62.7	16.922

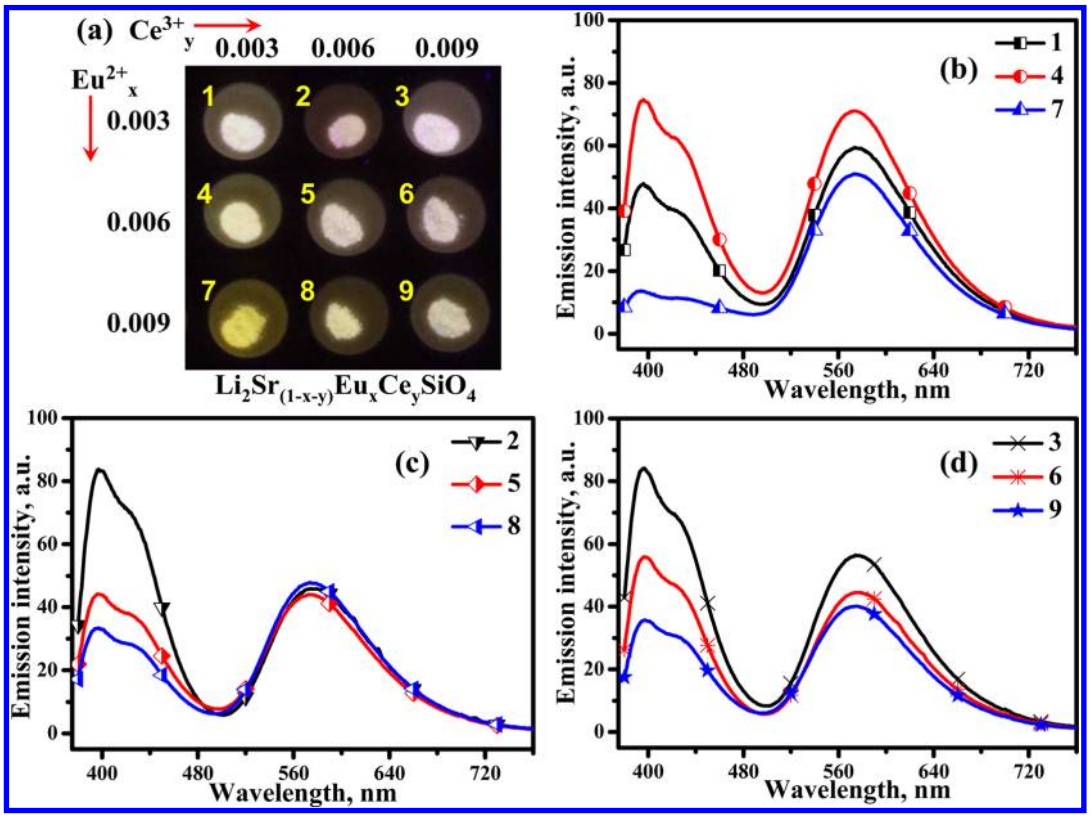

Figure 4. Composition map and luminescence photograph of combinatorial library and emission spectra of samples excited with 365 nm.

$Li_2(Sr_{1-x-y}Eu_xCe_y)SiO_4$, respectively. The chromaticity coordinates CIE(*x*, *y*), CRI, Tc, and the external QE of the 9 samples were provided in Table 1. The external QE reaches its maximum at the experiment 4 condition as $x = 0.006$ and $y = 0.003$ for $Li_2(Sr_{1-x-y}Eu_xCe_y)SiO_4$ and the Tc about 4058 K at this condition is appropriate, but the CRI about 64.9 is very low. The lowest Tc about 3272 K occurs under the experiment 7 condition ($x = 0.009$ for Eu^{2+} and $y = 0.003$ for Ce^{3+}), presenting warm white. The highest CRI about 69.4 occuring under the experiment 2 condition ($x = 0.003$ for Eu^{2+} and $y = 0.006$ for Ce^{3+}) is far below than the ordinary value about Ra 85 or more for home-lighting. The CIE (0.3714, 0.3310) under the experiment 6 condition is nearest to the standard CIE (0.3333, 0.3333) coordinates of white light. In short, the parameters that reflect the quality of emission color on LE, CRI, Tc, and chromaticity cannot reach their best values at one condition for the same Eu^{2+} and Ce^{3+} concentrations.

Figure 5 presents the CIE coordinates of the emission spectra of samples 2, 5, and 8, showing that luminescence color shifts from pure white to yellow white step by step with Eu^{2+} concentration increasing from $x = 0.003$ through 0.006 to 0.009 M as Ce^{3+} concentration is fixed on $y = 0.006$ M. Although the Tc of the emission at the experiment 8 condition is very warm, its CRI still is very low. Obviously, the emission spectrum is short of red component, as demonstrated with color purity analysis in the later. Otherwise, the CIE coordinates would shift toward the point of the triangle of red area.

To identify which factor combined with which level of concentration of Eu^{2+} and Ce^{3+} are most desirable for objective properties, the standard analysis by using the average values was adopted to perform the data process.[34] The "bigger-the-better" quality characteristic (QC) was selected for the analyses of LE and CRI, while the "smaller-the-better" QC is selected for the analysis of Tc. Figure 6a, b, and c shows the average values of

dx.doi.org/10.1021/co300058x | ACS Comb. Sci. 2012, 14, 636−644

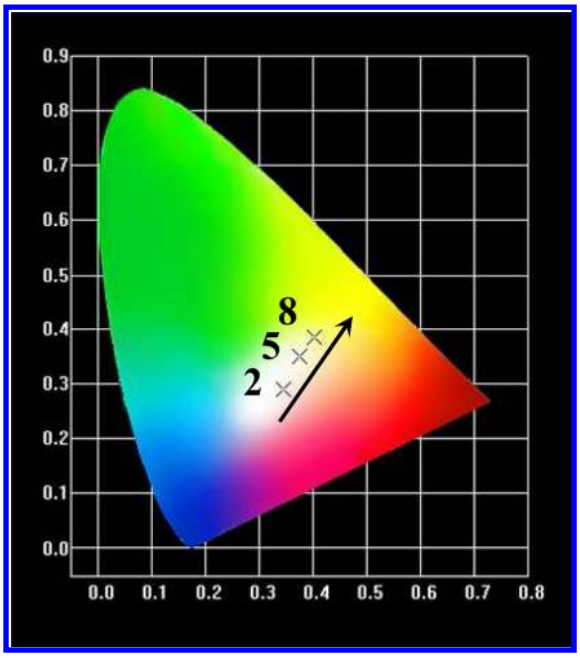

Figure 5. CIE coordinates of emission spectra of samples 2, 5, and 8.

each level of the control factors of Eu^{2+} and Ce^{3+} on the external QE, CRI, and Tc, respectively. The value of the external QE, CRI, and Tc vary significantly with Eu^{2+} concentration, showing that Eu^{2+} has great effect on them of all. Although the CRI and Tc change evidently with Ce^{3+} concentration varying, the external QE does not alter significantly with the variation of Ce^{3+} concentration, indicating that Ce^{3+} has great effect on CRI and Tc but has little effect on LE. Thus, the statistical analysis of variance (ANOVA) was conducted to determine the significance of control factors on the LE, CRI, and Tc. Table 2 presents the results of ANOVA for each factor. The last column in the ANOVA table shows the relative effects of factors on the objective properties.[34] The sum of all percentage effects including experimental error totals to 100%. A high percentage effect means that the factor has great impact on objective property or the factor tolerance must be monitored carefully.[34] As revealed in Table 2, the relative effects of the factor Eu^{2+} on the external QE, CRI, and Tc are about 49.64%, 62.88%, and 51.27%, respectively, while the effects of the factor Ce^{3+} on the external QE, CRI and Tc are about 11.19%, 18.01%, and 19.67%. Considering the interaction between Eu^{2+} and Ce^{3+} as a third or a fourth factor, as shown in the last column in Table 2, they have great impact on the objective properties. For example, the influence of the factor 4 (i.e., the INTRE COLS 2*1) on the external QE for whose effect is about 30.96% is far higher than the effect about 11.94% of Ce^{3+}, which discloses an important mechanism of luminescence about the energy transfer from Ce^{3+} to Eu^{2+}, as discussed in the following.

As far as the individual factor is concerned, the optimal level of concentration to achieve high LE, high CRI, and low Tc are 1 (0.003 M), 1 (0.003 M) and 3 (0.009 M) for the factor of Eu^{2+}, and 1 (0.003 M), 2 (0.006 M) and 1(0.003 M) or the factor Ce^{3+}, respectively. The contribution of factors at optimal condition to objective properties, the current grand average of performance, and the expected result at optimum conditions were disclosed in Supporting Information Table 1. However, the white light is produced by utilizing Eu^{2+} and Ce^{3+} emissions together. Therefore, the interaction between Eu^{2+} and Ce^{3+} has to be considered as a factor. The optimum levels of the interaction pairs between Eu^{2+} and Ce^{3+} on the external QE, CRI, and Tc were [2, 1], [1, 2], and [3, 1], respectively, and the corresponding severity indexes (SI) were 40.81%, 38.59%, and 29.56%. More details about these results were shown in Supporting Information Table 2. In mathematics, the 100% of SI indicates the angle between two lines is 90 degrees, and the 0% of SI means the two lines are parallel with each other. Therefore, the value about 40.81% and 38.59% of SI on the external QE and CRI suggests that the interaction between Eu^{2+} and Ce^{3+} are crucial to the objective properties. Moreover, the low value about 29.56% of SI on Tc can account for why the Tc has been very warm but the CRI is very low, for deficiency of some conponents in the binary Eu^{2+} and Ce^{3+} emission spectrum.

The above combinatorial optimization demonstrates that the sample at the Experiment-7 condition can emit warm white light, but perform poor CRI and low LE. Herewith, a scale-up synthesis of this sample was conducted to compare this one with commercially available LED phosphors. Figure 7 presents the emission spectra of the bulk sample of $Li_2(Sr_{0.985}Eu_{0.006}Ce_{0.009})SiO_4$ excited with 365 nm at 30−150 °C. By normalizing the initial luminescence intensity to 100, the relative intensity of Ce^{3+} emission at 412 nm and Eu^{2+} emission at 570 nm as a function of temperature were displayed in Figure 8, which shows that the decrease of Eu^{2+} emission upon temperature increasing is much more severe than that of Ce^{3+}, indicating that the thermal quench on Eu^{2+} emission is more severe than on Ce^{3+}. The luminescence intensity integrated from 380 to 730 nm and the relative luminance of the phosphor, which comprises both Ce^{3+} and Eu^{2+} full-spectrum emission after considering the effect of visual sensitivity function were also displayed in Figure.8. The decrease of luminance with an increase of temperature is more rapidly than that of the integrated intensity of luminescence. This is because the green dominates the composition of the white light, revealed by color purity analysis as shown in Table 3. Table 3 summarizes the variation of luminance, the external QE, chromaticity coordinates CIE (x, y), Tc, CRI, color purity (%), and the ratio of RGB in the white light of emission of the phosphor upon temperature. The LE and Tc become worse but the CRI gets better with an increase of temperature. Besides the poor thermal stability of luminescence, the external QE about 27.54% at room temperature is lower than that of the commercial phosphors, such as, about 81% for the red phosphor of $CaAlSiN:Eu^{2+}$, 74% for the yellow phosphor of YAG, 66% for the green phosphor of $Lu_3Al_5O_{12}:Ce^{3+}$ (LuAG), and 44% for the blue phosphor of $BaMgAl_{10}O_{17}:Eu^{2+}$ (BAM). Additionally, Figure.7 discloses a significant difference between the mechanism of Eu^{2+} and Ce^{3+}, where the emission spectra of Ce^{3+} red shifts but Eu^{2+} blue shifts with an increase of temperature. The red shift of emission spectrum usually is caused by the thermal vibration of electrons which intensifies with temperature increase. However, the blue shift of emission spectrum is caused by the phonon-coupling, in which the electrons are tuned from a low energy level to a higher one and then radiate light during electron transit from the high excited level to the ground state.

Finally, the excitation spectra were measured. The excitation spectra upon the emission of Eu^{2+} at 570 nm and the emission of Ce^{3+} at 418 nm of samples 2, 5, and 8 were displayed in Figure 9a and b, respectively. The wide band in the range of

dx.doi.org/10.1021/co300058x | ACS Comb. Sci. 2012, 14, 636−644

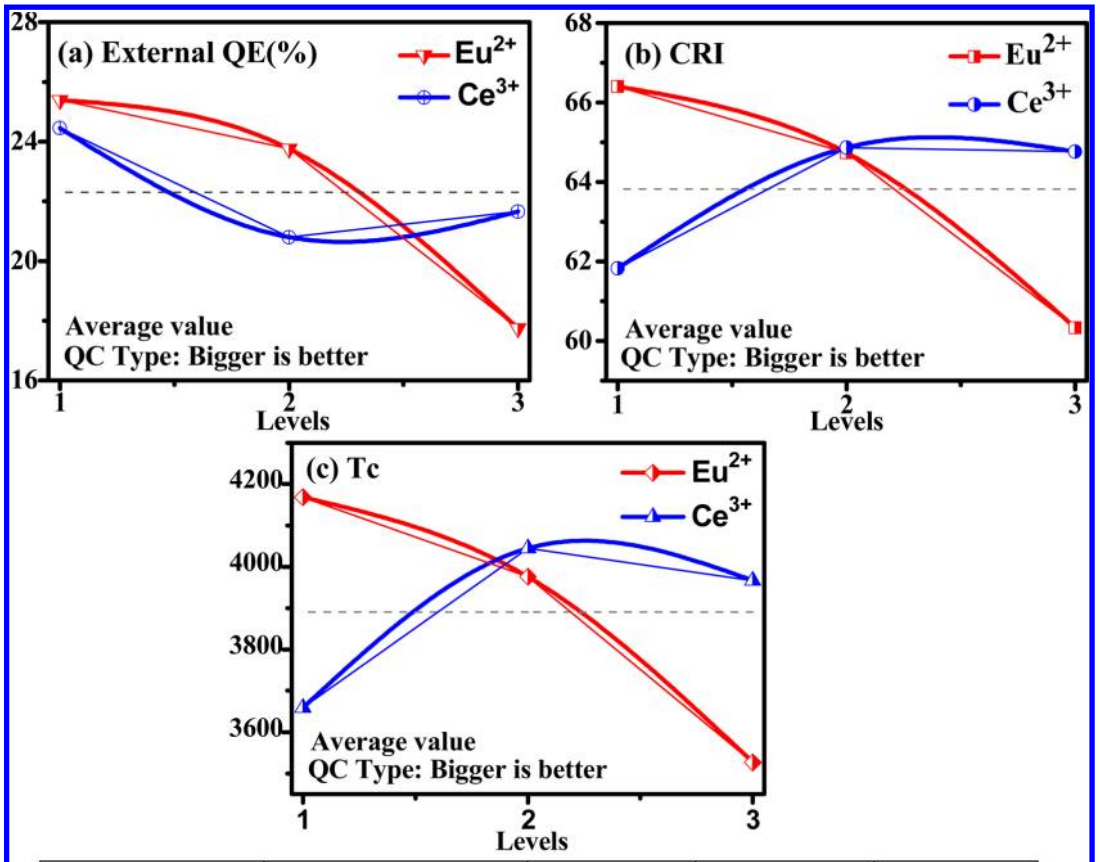

	Factors	Level 1	Level 2	Level 3
External QE (%)	1 Factor A (Eu^{2+})	25.394	23.76	17.75
	2 Factor B (Ce^{3+})	24.453	20.798	21.653
CRI (Ra)	1 Factor A (Eu^{2+})	66.4	64.733	60.333
	2 Factor B (Ce^{3+})	61.833	64.866	64.766
Tc (k)	1 Factor A (Eu^{2+})	4168	3975.666	3527
	2 Factor B (Ce^{3+})	3659.333	4044.666	3966.666

Figure 6. Average values of each level of the factors of Eu^{2+} and Ce^{3+} on the properties of relative luminescence efficiency (LE), color rendering index (CRI), and color temperature (Tc).

Table 2. Analysis of Variance (ANOVA) about the Significant Factors and Interaction Influences on Objective Properties

terms	column/factor	DOF (f)	sum of sqares (S)	variance (V)	pure sum (s)	percent P (%)
external QE (%)	1 factor Eu^{2+}	2	97.221	48.61	97.221	49.637
	2 factor Ce^{3+}	2	21.925	10.962	21.925	11.194
	3 inter cols 2 × 1	2	16.07	8.035	16.07	8.205
	4 inter cols 2 × 1	2	60.645	30.322	60.645	30.963
CRI	1 factor Eu^{2+}	2	58.942	29.471	58.942	62.881
	2 factor Ce^{3+}	2	17.816	8.908	17.816	18.006
	3 inter cols 2 × 1	2	16.113	8.056	16.113	17.189
	4 inter cols 2 × 1	2	0.858	0.429	0.858	0.915
Tc	1 factor Eu^{2+}	2	649176.83	324588.415	649176.83	51.27
	2 factor Ce^{3+}	2	249021.68	124510.84	249021.68	19.667
	3 inter cols 2 × 1	2	333756.549	166878.274	333756.549	26.359
	4 inter cols 2 × 1	2	34226.814	17113.407	34226.814	2.703

380−500 nm in Figure 9a was attributed to the f−d transition of Eu^{2+}; and the band in the range of 330−380 nm with a peak at 363 nm in Figure 9b was assigned to the f−d transition of Ce^{3+}. The presence of Ce^{3+} absorption in the excitation spectra of Eu^{2+} indicates that there is an energy transfer from Ce^{3+} to Eu^{2+}. Moreover, the excitation band of Eu^{2+} overlaps with the

dx.doi.org/10.1021/co300058x | ACS Comb. Sci. 2012, 14, 636−644

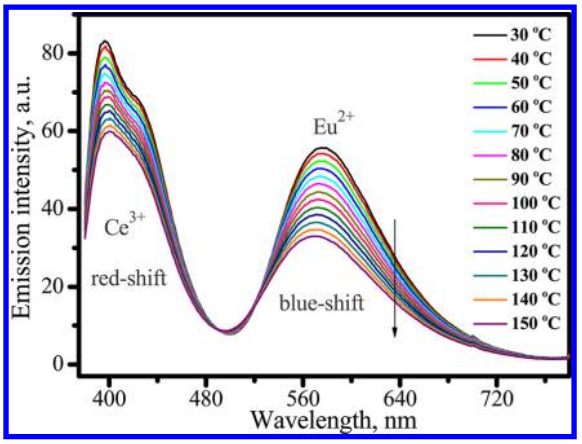

Figure 7. Emission spectra of $Li_2(Sr_{0.985}Eu_{0.006}Ce_{0.009})SiO_4$ excited with 365 nm at different temperature.

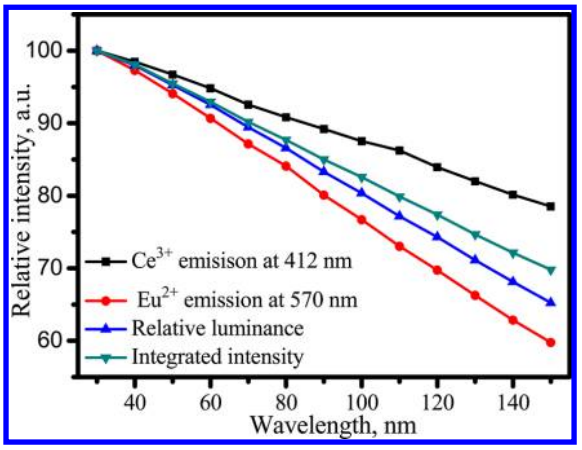

Figure 8. Normalized intensity of Ce^{3+} emission at 412 nm and Eu^{2+} emission at 570 nm and the overall luminescence intensity including both Ce^{3+} and Eu^{2+} integrated from 380 to 720 nm of $Li_2(Sr_{0.991}Eu_{0.006}Ce_{0.003})SiO_4$ as a function of temperature.

emission band of Ce^{3+}, as distinguished by comparing Figure 4 with Figure 9a. This point further demonstrates that there should exist in the energy transfer from Ce^{3+} to Eu^{2+}. The efficient energy transfer from Ce^{3+} to Eu^{2+} was observed in Fu's[40] experiment. However, the previous research reported by Kim pointed out that the energy transfer from Ce^{3+} to Eu^{2+} does not contribute to the enhancement of luminescence as for the Eu^{2+} and Ce^{3+} doubled-doped Li_2SrSiO_4 phosphor.[39]

If there were an efficient energy transfer from Ce^{3+} to Eu^{2+}, the luminescence intensity of Eu^{2+} should enhance correspondingly with Ce^{3+} content increasing before reaching to its critical concentration; and the increase of Eu^{2+} emission should at the expense of Ce^{3+} emission accordingly. Settled Ce^{3+} concentration at 0.003 M, Figure 4b shows that the luminescence of both Eu^{2+} and Ce^{3+} increases with Eu^{2+} increasing from 0.003 to 0.006 M, indicating that the concentrations of Eu^{2+} and Ce^{3+} at 0.003 M are lower than their critical concentrations. Another reasonable explanation was that a little Ce^{3+}-ion doping could stabilize the vacancies caused by Li^+ evaporation and inhibits the oxidization of Eu^{2+} to Eu^{3+}. Accordingly, the luminescence was improved.[39] When Ce^{3+} concentration was fixed to 0.006 M, Figure 4c shows that the intensity of Ce^{3+} decreases continuously with Eu^{2+} concentration increasing from 0.003 through 0.006 to 0.009 M, suggesting that the energy was transferred from Ce^{3+} to Eu^{2+}. But the luminescence of Eu^{2+} does not increase accordingly, maybe because the content of Eu^{2+} has reached to its critical concentration. To some extent, the energy could not be transferred from Ce^{3+} to Eu^{2+} efficiently. When the concentration of Ce^{3+} was 0.009 M, both Eu^{2+} and Ce^{3+} luminescence decrease with Eu^{2+} increasing from 0.003 to 0.009 M, because the concentrations of Ce^{3+}–Eu^{2+} are higher than their critical concentrations. Here, we can conclude that there is some energy transfer from Ce^{3+} to Eu^{2+} but that this energy transfer is not very efficient. Eu^{2+} and Ce^{3+} compete with each other to snatch the excitation energy during luminescence in the system of Eu^{2+}- and Ce^{3+}-codoped Li_2SrSiO_4. Eu^{2+} could emit by capturing excitation energy by itself, rather than depending on the energy transfer from Ce^{3+} to Eu^{2+}.

4. CONCLUSIONS

In summary, white light generation from the single-phased Li_2SrSiO_4 system was tuned up tailoring Eu^{2+} and Ce^{3+} concentrations. As far as the biggest contribution of individual

Table 3. Luminance, External Quantum Efficiency (QE), Chromaticity Coordinates (CIE (*x*, *y*)), Color Temperature (Tc), Color Purity, the Composition Ratio of RGB in White Light, and Color Rendering Index (CRI) of the Emission of the Phosphor $Li_2(Sr_{0.985}Eu_{0.006}Ce_{0.009})SiO_4$ as Function of Temperature

temp (°C)	lumin (cd/m²)	extern QE (%)	CIE *x*	CIE *y*	Tc (K)	color purity (%)	red percent (%)	green percent (%)	blue percent (%)	CRI (Ra)
30	100	27.54	0.359	0.314	4188	7.8	18.6	78.6	2.9	66.8
40	97.98	27.00	0.3576	0.314	4248	7.6	18.4	78.7	2.9	67.1
50	95.26	26.26	0.3556	0.314	4336	7.2	18.2	78.9	2.9	67.5
60	92.53	25.55	0.3535	0.3137	4427	6.9	18	79	3	68
70	89.45	24.77	0.3514	0.3131	4523	8.1	17.8	79.1	3	68.5
80	86.60	24.07	0.3492	0.3122	4617	7.9	17.7	79.2	3.1	69
90	83.30	23.29	0.3465	0.3107	4739	7.9	17.5	79.3	3.2	69.7
100	80.36	22.59	0.3439	0.3094	4865	7.9	17.3	79.4	3.3	70.3
110	77.18	21.82	0.3409	0.3079	5013	8	17.1	79.5	3.3	70.8
120	74.28	21.10	0.338	0.3065	5166	8.2	16.9	79.7	3.4	71.5
130	71.11	20.33	0.3349	0.3047	5336	8.6	16.7	79.8	3.5	72.1
140	68.12	19.60	0.3318	0.3027	5521	8.4	16.5	79.9	3.6	72.7
150	65.25	18.92	0.3287	0.3004	5712	9.1	16.3	80	3.7	73.3

dx.doi.org/10.1021/co300058x | ACS Comb. Sci. 2012, 14, 636–644

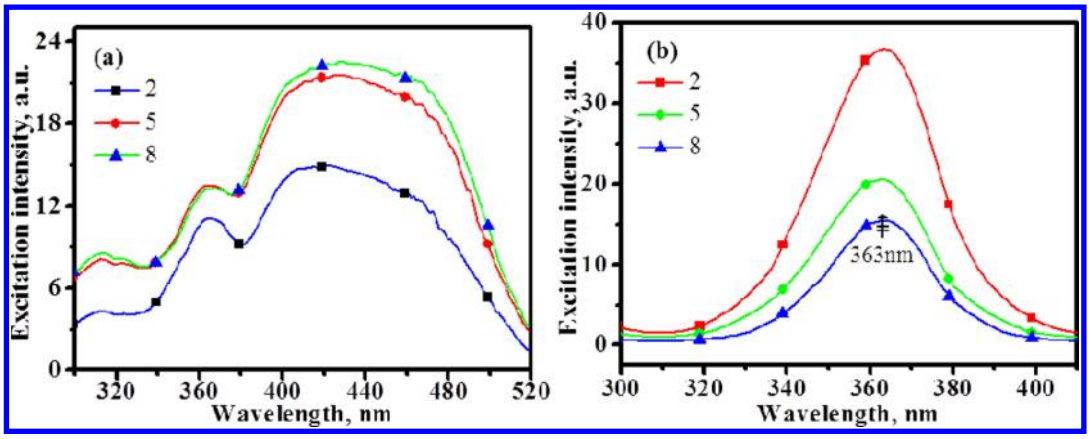

Figure 9. Excitation spectra of samples 2, 5, and 8.

factor on objective properties is concerned, the optimum concentration to achieve high luminescence efficiency, high color rendering index, and low correlated color temperature are 0.003 M, 0.003 M, and 0.009 M for the factor of Eu^{2+} and 0.003 M, 0.006 M, and 0.003 M for the factor of Ce^{3+}, respectively respectively. The interaction pairs between Eu^{2+} and Ce^{3+} were processed as a factor to obtain the best performance in terms of high luminescence efficiency, high color rendering index, and low correlated color temperature: the optimum concentration is (0.006 M, 0.003 M), (0.003 M, 0.006), and (0.009 M, 0.003 M). The phosphor performs low thermal stability of luminescence and poor color rendering ability. The luminance of $Li_2(Sr_{0.985}Eu_{0.006}Ce_{0.009})SiO_4$. emission under 365 nm excitation losses about 35% with temperature increasing from 30 to 150 °C. The emission of Ce^{3+} red shifts, while the emission of Eu^{2+} blue shifts with an increase of temperature, which results in the color rendering ability get better with temperature increasing although the luminescence efficiency and correlated color temperature become worse. The analyses by using the Taguchi method reveals that Eu^{2+} and Ce^{3+} have different effects on the objective properties of luminescence efficiency, color rendering index, and color temperature, which provides an important clue to understand the mechanism of luminescence and accounts for why the parameters of the objective properties cannot maximize at the same one concentration of Eu^{2+} and Ce^{3+}. The value of low severity index between Eu^{2+} and Ce^{3+} interaction on luminescence intensity indicates the energy could not transfer from Ce^{3+} to Eu^{2+} efficiently, where Eu^{2+} and Ce^{3+} compete with each other to snatch the excitation energy. Eu^{2+} could emit by capturing excitation by itself, rather than depending on the energy transfer. The low severity index between Eu^{2+} and Ce^{3+} on the color rendering index suggests that the spectrum comprises of Eu^{2+} and Ce^{3+} emission was deficient in red and blue components, demonstrated with color purity calculation.

■ ASSOCIATED CONTENT

Supporting Information

Emission spectra of some samples in combinatorial library, their integrated intensity of luminescence, the three-dimensional crystal structure, optimum conditions and performance of different factors, their interaction, and optimal levels achieved by calculating with the Taguchi method. This material is available free of charge via the Internet at http://pubs.acs.org.

■ AUTHOR INFORMATION

Corresponding Author

*E-mail: chichengfeiyang@yahoo.com.cn (L.C.); chshifu@chnu.edu.cn (S.-F.C.). Phone: +86-551-2904566 (L.C.); +86-561-3606611 (S.-F.C.).

Funding

The authors acknowledge the financial support from the National High-Tech R&D Program of China (863 program) for semiconductor lighting application and demonstration of "Ten cities with all LED lamps", the National Natural Science Foundation of China (No.s 51002043, 51172086, and 61076040), the Science Foundation for Excellent Young Scholars of the Ministry of Education of China (No. 20090111120001), the Key Technology Research and Development of Anhui Province (No. 12010202004), China Postdoctoral Science Foundation (No. 20090450802 and 2012T50568), and the Student Innovation Training Program of Hefei University of Technology (No.s XS11121 and 2012CXCY044).

Notes

The authors declare no competing financial interest.

■ REFERENCES

(1) Schubert, E. F.; Kim, J. K. Solid-state light sources getting smart. *Science* **2005**, *308*, 1274−1278.

(2) Ye, S.; Xiao, F.; Pan, Y.; Ma, Y.; Zhang, Q. Phosphors in phosphor-converted white light-emitting diodes: Recent advances in materials, techniques and properties. *Mater. Sci. Eng., R* **2010**, *71*, 1−34.

(3) Xie, R.-J.; Hirosaki, N. Silicon-based oxynitride and nitride phosphors for white LEDs—A review. *Sci. Technol. Adv. Mater.* **2007**, *8*, 588−600.

(4) Chen, L.; Lin, C. C.; Yeh, C. W.; Liu, R. S. Light converting inorganic phosphors for white light-emitting diodes. *Materials* **2010**, *3*, 2172−2195.

(5) Jeong, H. H.; Lee, S. Y.; Choi, K. K.; Song, J. O.; Lee, J. H.; Seong, T. Y. Enhancement of light output power of GaN-based vertical light emitting diodes by optimizing *n*-GaN thickness. *Microelectron. Eng.* **2011**, *88*, 3164−3167.

(6) Zhmakin, A. I. Enhancement of light extraction from light emitting diodes. *Phys. Rep.* **2011**, *498*, 189−241.

(7) Pearsall, T.; Roussel, P.; Berlitz, S.; Heider, C.; Winkler, H.; Enderle, H.; Kuehn, C.; Petry, R.; Vosgroene, T.; Pohlmann, W. *Manuf. LEDs Light. Disp., Proc.* **2007**, *6797*, 0I−12.

(8) Yang, C. C.; Chang, C. L.; Huang, K. C.; Liao, T. S. The yellow ring measurement for the phosphor-converted white LED. *Phys. Proc.* **2011**, *19*, 182−187.

(9) Nakamura, S.; Fasol, G. *The Blue Laser Diode: GaN Based Blue Light Emitters and Lasers*; Springer, Berlin: 1997,pp 216.
(10) Sheu, J. K.; Chang, S. J.; Kuo, C.; Su, Y. K.; Wu, L.; Lin, Y.; Lai, W.; Tsai, J.; Chi, G. C.; Wu, R. White-light emission from near UV InGaN−GaN LED chip precoated with blue/green/red phosphors. *IEEE Photonics Technol. Lett.* **2003**, *15*, 18−20.
(11) Chen, L.; Chu, C. I.; Liu, R. S. Improvement of emission efficiency and color rendering of high-power LED by controlling size of phosphor particles and utilization of different phosphors. *Microelectron. Reliab.* **2011**, *52*, 900−904.
(12) Chen, L.; Chen, K. J.; Hu, S. F.; Liu, R. S. Combinatorial chemistry approach to searching phosphors for white light-emitting diodes in (Gd-Y-Bi-Eu) VO4 quaternary system. *J. Mater. Chem.* **2011**, *21*, 3677−3685.
(13) Huang, C. H.; Chen, T. M. A novel single-composition trichromatic white-light $Ca_3Y(GaO)_3(BO_3)_4$:Ce^{3+}, Mn^{2+}, Tb^{3+} phosphor for UV-light emitting diodes. *J. Phys. Chem. C.* **2011**, *115*, 2349−2355.
(14) Saradhi, M. P.; Varadaraju, U. Photoluminescence studies on Eu^{2+}-activated Li_2SrSiO_4: A potential orange-yellow phosphor for solid-state lighting. *Chem. Mater.* **2006**, *18*, 5267−5272.
(15) Kulshreshtha, C.; Sharma, A. K.; Sohn, K.-S. Effect of local structures on the luminescence of $Li_2(Sr,Ca,Ba)SiO_4$:Eu^2. *J. Electrochem. Soc.* **2009**, *156*, J52.
(16) Dotsenko, V. P.; Levshov, S. M.; Berezovskaya, I. V.; Stryganyuk, G. B.; Voloshinovskii, A. S.; Efryushina, N. P. Luminescent properties of Eu^{2+} and Ce^{3+} ions in strontium litho-silicate Li_2SrSiO_4. *J. Lumin.* **2011**, *131*, 310−315.
(17) Zhang, X.; He, H.; Li, Z.; Yu, T.; Zou, Z. Photoluminescence studies on Eu^{2+} and Ce^{3+}-doped Li_2SrSiO_4. *J. Lumin.* **2008**, *128*, 1876−1879.
(18) Xiang, X. D.; Sun, X.; Briceno, G.; Lou, Y.; Wang, K. A.; Chang, H.; Wallace-Freedman, W. G.; Chen, S. W.; Schultz, P. G. A combinatorial approach to materials discovery. *Science* **1995**, *268*, 1738−1740.
(19) Briceno, G.; Chang, H.; Sun, X.; Schultz, P. G.; Xiang, X. D. A class of cobalt oxide magnetoresistance materials discovered with combinatorial synthesis. *Science* **1995**, *270*, 273−275.
(20) Janda, K. D.; Lo, L. C.; Lo, C. H. L.; Sim, M. M.; Wang, R.; Wong, C. H.; Lerner, R. A. Chemical selection for catalysis in combinatorial antibody libraries. *Science* **1997**, *275*, 945−948.
(21) Reddington, E.; Sapienza, A.; Gurau, B.; Viswanathan, R.; Sarangapani, S.; Smotkin, E. S.; Mallouk, T. E. Combinatorial electrochemistry: A highly parallel, optical screening method for discovery of better electrocatalysts. *Science* **1998**, *280*, 1735−1737.
(22) Danielson, E.; Golden, J. H.; McFarland, E. W.; Reaves, C. M.; Weinberg, W. H.; Di Wu, X. A combinatorial approach to the discovery and optimization of luminescent materials. *Nature* **1997**, *389*, 944−948.
(23) Wang, J.; Yoo, Y.; Gao, C.; Takeuchi, I.; Sun, X.; Chang, H.; Xiang, X. D.; Schultz, P. G. Identification of a blue photoluminescent composite material from a combinatorial library. *Science* **1998**, *279*, 1712−1714.
(24) Danielson, E.; Devenney, M.; Giaquinta, D. M.; Golden, J. H.; Haushalter, R. C.; McFarland, E. W.; Poojary, D. M.; Reaves, C. M.; Weinberg, W. H.; Di Wu, X. A rare-earth phosphor containing one-dimensional chains identified through combinatorial methods. *Science* **1998**, *279*, 837−839.
(25) Olender, R.; Rosenfeld, R. A fast algorithm for searching for molecules containing a pharmacophore in very large virtual combinatorial libraries. *J. Chem. Inf. Comput. Sci.* **2001**, *41*, 731−738.
(26) Gillet, V. J.; Khatib, W.; Willett, P.; Fleming, P. J.; Green, D. V. S. Combinatorial library design using a multiobjective genetic algorithm. *J. Chem. Inf. Comput. Sci.* **2002**, *42*, 375−385.
(27) Young, S. S.; Wang, M.; Gu, F. Design of diverse and focused combinatorial libraries using an alternating algorithm. *J. Chem. Inf. Comput. Sci.* **2003**, *43*, 1916−1921.
(28) Reynolds, C. H.; Tropsha, A.; Pfahler, L. B.; Druker, R.; Chakravorty, S.; Ethiraj, G.; Zheng, W. Diversity and coverage of structural sublibraries selected using the SAGE and SCA algorithms. *J. Chem. Inf. Comput. Sci.* **2001**, *41*, 1470−1477.
(29) Weber, L. Applications of genetic algorithms in molecular diversity. *Curr. Opin. Chem. Biol.* **1998**, *2*, 381−385.
(30) Schneider, G.; Wrede, P. Artificial neural networks for computer-based molecular design. *Prog. Biophys. Mol. Biol.* **1998**, *70*, 175−222.
(31) Sohn, K. S.; Park, D. H.; Cho, S. H.; Kim, B. I.; Woo, S. I. Genetic algorithm-assisted combinatorial search for a new green phosphor for use in tricolor white LEDs. *J. Comb. Chem.* **2006**, *8*, 44−49.
(32) Sohn, K. S.; Park, D. H.; Cho, S. H.; Kwak, J. S.; Kim, J. S. Computational evolutionary optimization of red phosphor for use in tricolor white LEDs. *Chem. Mater.* **2006**, *18*, 1768−1772.
(33) Jung, Y. S.; Kulshreshtha, C.; Kim, J. S.; Shin, N.; Sohn, K. S. Genetic algorithm-assisted combinatorial search for new blue phosphors in a $(Ca, Sr, Ba, Mg, Eu)_xB_yP_zO_\delta$ System. *Chem. Mater.* **2007**, *19*, 5309−5318.
(34) Chen, L.; Chu, C. I.; Chen, K. J.; Chen, P. Y.; Hu, S. F.; Liu, R. S. An intelligent approach to the discovery of luminescent materials using a combinatorial approach combined with Taguchi methodology. *J. Lumin.* **2011**, *26*, 229−238.
(35) Chen, L.; Chen, K. J.; Lin, C. C.; Chu, C. I.; Hu, S. F.; Lee, M. H.; Liu, R. S. Combinatorial approach to the development of a single mass YVO_4: Bi^{3+}, Eu^{3+} phosphor with red and green dual colors for high color rendering white light-emitting diodes. *J. Comb. Chem.* **2010**, *12*, 587−594.
(36) Chen, L.; Bao, J.; Gao, C.; Huang, S.; Liu, C.; Liu, W. Combinatorial synthesis of insoluble oxide library from ultrafine/nano particle suspension using a drop-on-demand inkjet delivery system. *J. Comb. Chem.* **2004**, *6*, 699−702.
(37) Chen, L.; Fu, Y.; Zhang, G.; Bao, J.; Gao, C. Optimization of Pr^{3+}, Tb^{3+}, and Sm^{3+} Co-doped $(Y_{0.65}Gd_{0.35})$ BO_3: $Eu_{0.05}{}^{3+}$ VUV phosphors through combinatorial approach. *J. Comb. Chem.* **2008**, *10*, 401−404.
(38) Roy, R. *Qualitek-4. Software for Automatic Design and Analysis of Taguchi Experiments*; Nutek, Inc.: Bloomfield Hills, MI, U.S.A., 2007.
(39) Kim, T.-G.; Lee, H.-S.; Lin, C. C.; Kim, T.; Liu, R.-S.; Chan, T.-S.; Im, S.-J. Effects of additional Ce^{3+}-doping on the luminescence of Li_2SrSiO_4:Eu^{2+} yellow phosphor. *Appl. Phys. Lett.* **2010**, *96*, 061904−3.
(40) He, H.; Fu, R. L.; Cao, Y. G.; Song, X. F.; Pan, Z. W.; Zhao, X. R.; Xiao, Q. B.; Li, R. $Ce^{3+} \rightarrow Eu^{2+}$ energy transfer mechanism in the Li_2SrSiO_4:Eu^{2+}, Ce^{3+} phosphor. *Opt. Mater.* **2010**, *32*, 632−636.